Adiabaticity Engineered Silicon Polarization Independent 3-dB Coupler for the O-Band

Hung-Ching Chung, Chih-Hsien Chen, Guan-Xun Lu, Yung-Jr Hung, *Member, IEEE*, and Shuo-Yen Tseng, *Member, IEEE*

***Abstract*—We demonstrate a compact and broadband polarization independent 3-dB coupler for the O-band on silicon-on-insulator platform. Using the multi-parameter adiabaticity engineering protocol, unwanted coupling between eigenmodes in mode evolution couplers are redistributed for dual polarization modes and multiple wavelengths, resulting in a large operating bandwidth for both TE and TM polarizations. The fabricated device has a bandwidth of 70 nm with a compact mode evolution region of 27 μm.**

***Index Terms*—Integrated photonics circuit, silicon photonics, waveguides, adiabatic coupler.**

I. Introduction

OWING to its ability to be easily integrated with complementary metal-oxide-semiconductor (CMOS) manufacturing processes [1] and the potential to achieve electronic-photonics integration [2], silicon photonics has been widely used in photonic integrated circuits (PICs). Moreover, the signature of high refractive index contrast between core and cladding on silicon-on-insulator (SOI) platform enables large-scale and high-density photonic integration on a chip. Optical 3-dB couplers with wide bandwidth are essential components in photonic integrated PICs and find frequent applications in optical switching. [3], modulators [4] and multiplexers [5]. However, high refractive index contrast also causes birefringence of the silicon waveguides, resulting in polarization-dependent silicon photonic devices. That is, the coupling strengths of TE and TM polarized light are quite different in silicon waveguide power couplers and splitters [6]. Broadband and polarization-independent 3-dB couplers are necessary and desirable for applications that demand polarization diversity. Many types of polarization-independent 3-dB couplers had been proposed. Subwavelength grating waveguides have been used to realize polarization-independent 3-dB couplers with compact size and large bandwidth [7], [8]. Nevertheless, subwavelength grating waveguide needs precise structure control, so electron-beam lithography process is often required for device fabrication. Polarization-independent 3-dB coupler designs based on mode evolution had been developed [9], but their mode evolution regions are relatively long (75 μm) due to the adiabatic designs. Bent waveguide couplers were utilized to achieve broadband polarization-independent 3-dB couplers [10]. However, the design of cascaded bent couplers also requires high fabrication precision. It is worth noting that the aforementioned devices are all designed and experimentally realized for the C-band wavelengths. To our best knowledge, there are limited efforts on the design and fabrication of polarization-independent 3-dB couplers for the O-band.

Research has been conducted over the years to explore the similarities and analogies between quantum mechanics and wave optics [11]. An example of the analogy is the similarity between the Schrödinger equation for two-level systems in quantum mechanics and the coupled-mode equation in wave optics. Thanks to this analogy, the techniques in quantum mechanics can be applied in optical waveguide couplers. A family of protocols called shortcuts to adiabaticity (STA) has also found analogies in coupled waveguide devices, resulting in short and robust integrated optics components [12], [13]. Short and broadband 3-dB couplers have been designed and experimentally demonstrated using a STA called fast quasi-adiabatic dynamics (FAQUAD) [14]. However, the FAQUAD strategy can cause large differences in the adiabaticity parameters between TE and TM mode, so the coupler could be made transparent to the TM mode but functions as a 3-dB coupler for the TE mode [15]. In other words, the FAQUAD strategy can only manipulate a single-mode system. A polarization-independent silicon 3-dB coupler for the C-band was realized using FAQUAD under the quasi-adiabatic regime [16], where only one of the polarization modes works under adiabatic regime and the other under mode coupling regime. Previously, we have proposed an adiabaticity engineering (AE) technique that can manipulate multi-mode

Manuscript received 27 March 2023; revised 21 April 2023; accepted 26 April 2023. Date of publication 28 April 2023; date of current version 5 May 2023. This work was supported in part by the Ministry of Science and Technology, Taiwan under Grants 111-2221-E-006-052-MY3 and 109-2221-E-110-068-MY3 and in part by Higher Education SPROUT project, Ministry of Education, Taiwan. *(Corresponding authors: Yung-Jr Hung; Shuo-Yen Tseng.)*

Hung-Ching Chung and Guan-Xun Lu are with the Department of Photonics, National Cheng Kung University, Tainan 701, Taiwan (e-mail: fonpy78031075@gmail.com; gary860610@gmail.com).

Chih-Hsien Chen is with the Department of Photonics and the Miniaturized Photonic Gyroscope Research Center, National Sun Yat-sen University, Kaohsiung 804, Taiwan (e-mail: chenhsien0417@gmail.com).

Yung-Jr Hung is with the Department of Photonics and the Miniaturized Photonic Gyroscope Research Center, National Sun Yat-sen University, Kaohsiung 804, Taiwan (e-mail: yungjr@mail.nsysu.edu.tw).

Shuo-Yen Tseng is with the Department of Photonics, National Cheng Kung University, Tainan 701, Taiwan, and also with the Miniaturized Photonic Gyroscope Research Center, National Sun Yat-sen University, Kaohsiung 804, Taiwan (e-mail: tsengsy@mail.ncku.edu.tw).

Digital Object Identifier 10.1109/JPHOT.2023.3271320

systems, and we have applied multi-mode AE to design a compact and broadband polarization-independent 3-dB coupler [17]. Recently, we developed a multi-wavelength AE that further improves the operation bandwidth of the resulting photonic devices [18]. In particular, the multi-wavelength AE allows us to select the wavelength range of operation for enhancing the device bandwidth. Nevertheless, these works on adiabaticity engineering were limited to theoretical studies and simulations.

In this paper, we design and fabricate broadband polarization-independent 3-dB couplers for the O-band using a combination of multi-mode AE and multi-wavelength AE. This new technique is called the multi-parameter adiabaticity engineering (MPAE), which was previously used for the design of a C-band polarization-independent 3-dB coupler [19]. In this work, MPAE is used to optimize the mode evolution region of silicon adiabatic 3-dB couplers for dual polarization modes and multiple wavelengths. We report a compact and broadband polarization independent 3-dB coupler realized using a multiple project wafer (MPW) foundry service. The device mode evolution region is 27 μm, and the measured polarization independent bandwidth is over 70 nm ranging from 1270 to 1340 nm.

II. Multi-Parameter Adiabaticity Engineering

In this section, we introduce a technique to optimize device adiabatic metric over dual polarization modes and multiple wavelengths by a single control parameter. Defining the adiabaticity metric in optical waveguides has been a subject of many works [20], [21], [22]. In this paper, we follow the heuristic approach in [23] and define the adiabaticity parameter C in an optical waveguide as

$$C\ (z) = \frac{\langle m|\ \frac{d}{dz}\ |n\rangle}{\beta_m - \beta_n} = \frac{dz}{dW}\ \frac{\langle m|\ \frac{d}{dW}\ |n\rangle}{\beta_m - \beta_n} = \frac{1}{R\,(W)}\ F\,(W) \tag{1}$$

where $|m, n\rangle$ are the eigenmodes of an optical waveguide, $\beta_{m,n}$ are the propagation constants of the eigenmodes, W is the control parameter (corresponding to waveguide width in our design example which will be discussed in Section III). F(W) is solely dependent on the control parameter W. If the geometry and material composition of the waveguide cross-section is determined, $F(W)$ would be a fixed function of W. With the assumption of W being monotonically increasing ($dW/dz > 0$), $R(W)$ defines the rate at which z changes with W. The adiabaticity parameter C presents a measure of the degree of coupling between eigenmode $|m\rangle$ and eigenmode $|n\rangle$. From (1), we find that the adiabaticity parameter C can be engineered through the rate of change $R(W)$. Hence, the concept underlying MPAE involves engineering the most suitable distribution of $R(W)$ to minimize the aggregate unwanted coupling in multi-mode and multi-wavelength systems.

To ensure wideband functionality, the initial step involves separate design of $R(W)$ for TE and TM polarizations, $R_{TE}(W)$ and $R_{TM}(W)$, by accounting for contributions from multiple wavelengths. To realize a polarization-independent 3-dB coupler for the O-band, we choose three wavelengths, 1210 nm, 1310 nm and 1410 nm, so that the resulting bandwidth covers the entire O-band spectral region. For each wavelength λ, $R_\lambda(W)$ represents the optimal rate of change that evenly distributes adiabaticity along the evolution. A larger $R_\lambda(W)$ value indicates that the control parameter W needs to be varied slower with z, and vice versa. When multiple wavelengths are considered, we engineer the overall $R(W)$ by considering contributions from each wavelength. At each W, we determine $R(W)$ by selecting the largest $R_\lambda(W)$ as it indicates the largest unwanted coupling among the wavelengths. The condition we impose on $R(W)$'s can thus be expressed as:

$$\begin{aligned} &R_{TE,TM}\,(W) \\ &= \max\{\ r_1 R_{1210}\,(W), r_2 R_{1310}\,(W), r_3 R_{1410}\,(W)\} \end{aligned} \tag{2}$$

where weights r_1, r_2 and r_3 are assigned to each wavelength, dictating their respective contributions and $r_1 + r_2 + r_3 = 1$. Using (2), the optimal distributions for broadband operation are first determined for the TE and TM polarizations, respectively.

Using a similar approach, polarization independence can be obtained by designing $R_{AE}(W)$ for both TE and TM modes, while ensuring the following condition is met:

$$R_{AE}\,(W)\ = \max\{\ r_{TE} R_{TE}\,(W), r_{TM} R_{TM}\,(W)\} \tag{3}$$

where the TE and TM mode weights, denoted as r_{TE} and r_{TM}, determine their respective contributions and $r_{\mathrm{TE}} + r_{\mathrm{TM}} = 1$.

Fig. 1 illustrates the schematic steps involved in MPAE. Firstly, we calculate $C(z)$ for TE and TM modes at 1210 nm, 1310 nm, and 1410 nm, with W varying linearly (dW/dz = constant) [Fig. 1(a)]. We can then find $R_{1210}(W)$, $R_{1310}(W)$, and $R_{1410}(W)$, which evenly distribute adiabaticity at their respective wavelengths. We then optimize the weights r_1, r_2 and r_3, in (2) for broadband operation [Fig. 1(b)]. Once $R_{TE}(W)$ and $R_{TM}(W)$ are determined using (2) for a specific set of r_1, r_2, and r_3, illustrated by the purple curves in Fig. 1(b), we can calculate the updated $C(z)$'s for TE and TM modes as shown in Fig. 1(c), which represent the adiabaticity parameters corresponding to the engineered $R_{TE}(W)$ and $R_{TM}(W)$ at the chosen wavelengths. The main objective of MPAE is to minimize the total unwanted coupling by minimizing the sum of the maxima of $C(z)$'s [red circles in Fig. 1(c)], denoted as $\sum_\lambda \max_z\{C(z)\}$, through the weights r_1, r_2, and r_3. Through a systematic search of all parameters, we obtain $r_1 = 0.34$, $r_2 = 0.37$, $r_3 = 0.29$ for the TE polarization and $r_1 = 0.33$, $r_2 = 0.36$, $r_3 = 0.31$ for the TM polarization, achieving the minimum $\sum_\lambda \max\{C(z)\}$ for both polarizations.

After obtaining $R_{TE}(W)$ and $R_{TM}(W)$, the optimization process is repeated to engineer $R_{AE}(W)$ for polarization independence operation, by minimizing $\sum_{TE,TM} \max_z\{C(z)\}$ through the weights r_{TE} and r_{TM} in (3). The values of r_{TE} and r_{TM} are found to be 0.64 and 0.36, respectively. The yellow curve in Fig. 1(e) shows the corresponding optimal $R_{AE}(W)$,

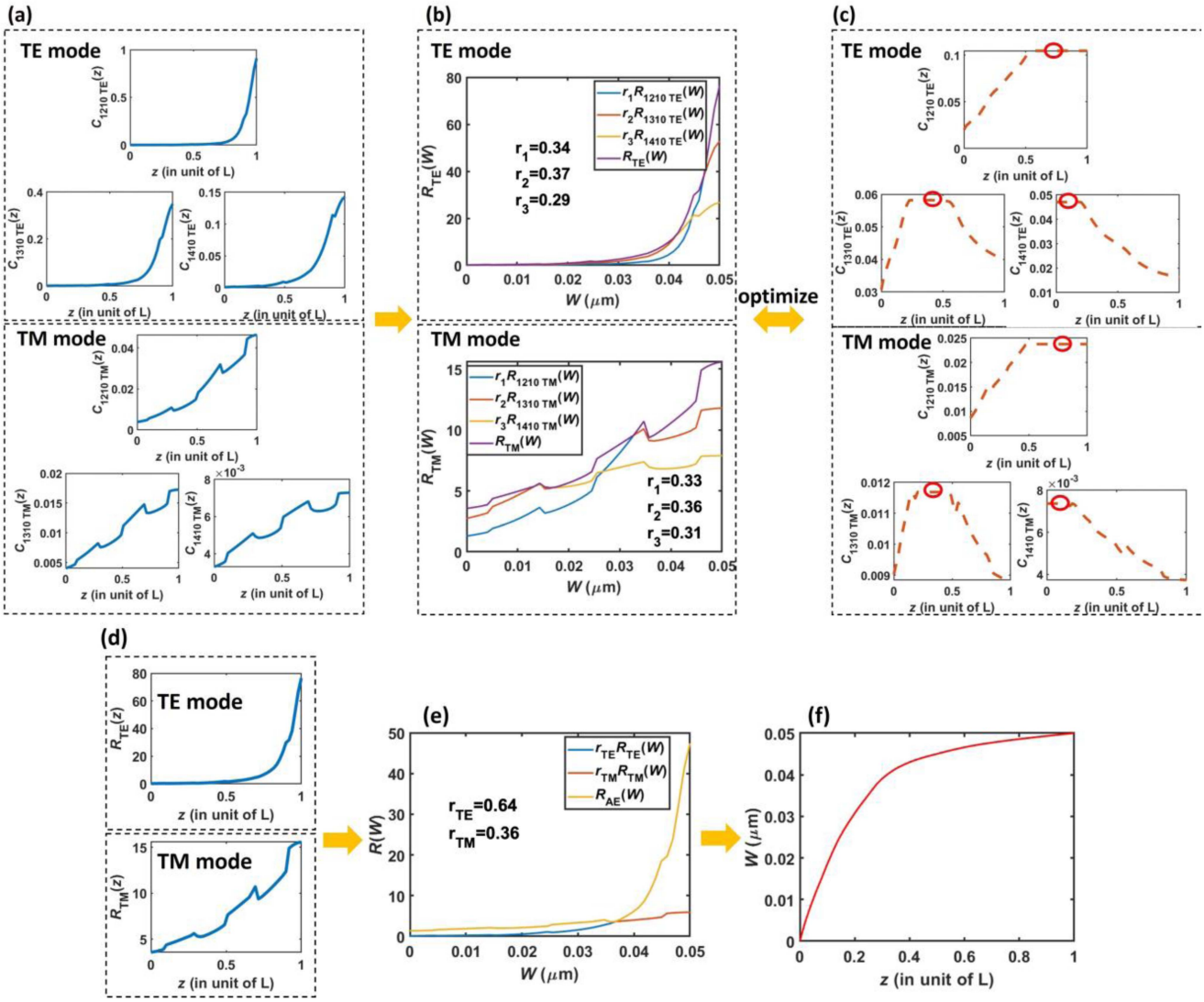

Fig. 1. The steps involved in multi-parameter adiabaticity engineering (MPAE) are depicted in the schematic diagram. The first step involves obtaining the adiabaticity parameters for both TE and TM modes in a device with linear variation. Subsequently, in steps (b) and (c), the contributions from three wavelengths are optimized to minimize undesirable coupling for TE and TM modes, respectively. In steps (d) and (e), the weights for both polarizations are optimized to minimize the overall unwanted coupling. Finally, in step (f), the MPAE-optimized structure is obtained by integration.

which minimizes the overall adiabaticity parameter and reduces unwanted coupling. The control parameter $W(z)$ can be obtained by integrating both sides of the equation $1/R_{AE}(W) = \mathrm{d}W/\mathrm{d}z$ [Fig. 1(f)], completing the MPAE procedure.

III. Design and Simulation

Our design for the polarization-independent 3-dB coupler considers an SOI substrate with a top silicon layer thickness of 220 nm and a buried oxide layer thickness of 2 μm. The cladding layer in our design is silica, as illustrated in Fig. 2(a). Fig. 2(b) presents the top view schematic of the MPAE-optimized polarization-independent 3-dB coupler. $W(z)$ corresponds to the control parameter introduced in the previous section. The input and output width W_0 of MPAE-optimized polarization-independent 3-dB coupler is chosen to be 0.38 μm to match the width specification of single-mode SOI waveguide for O-band. In the 5-μm long region I, the upper optical path consists of a linear taper waveguide with width varying from $W_0 = 0.38$ μm to $W_1 = 0.4$ μm, and the lower optical path is a taper waveguide with width varying from $W_0 = 0.38$ μm to $W_2 = 0.3$ μm. The gap g_1 is 3 μm. In the 20-μm long region II, we employ two S-bend waveguides of widths W_1 and W_2 to bring the two waveguides together ($g_1 = 3$ μm $\rightarrow$ $g_2 = 0.15$ μm). Region III is the mode evolution region of MPAE-optimized polarization-independent 3-dB coupler. Though a constant gap of g_2 is maintained, a taper function $W(z)$ designed by MPAE is applied to both waveguides so that their widths become $W_1(z) = W_1 - W(z)$ and $W_2(z) = W_2 + W(z)$. $W(z)$ is varied from 0 to 0.05 μm, and width W_3 for both waveguides at the end of region III is 0.35 μm. The taper function $W(z)$ and length L of Region III is optimized by setting $W(z)$ as the control parameter in (1).

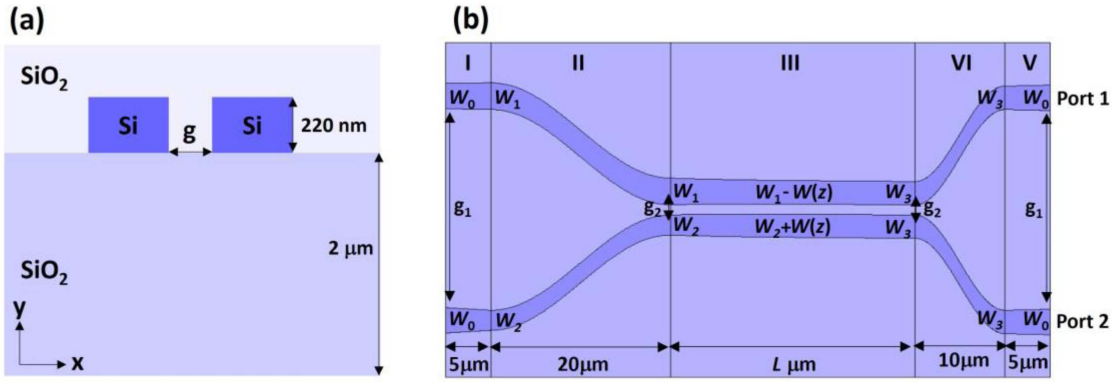

Fig. 2. Schematics of the MPAE-optimized 3-dB coupler (a) Cross-sectional view. (b) Top view. $W(z)$ is the control parameter for adiabaticity engineering.

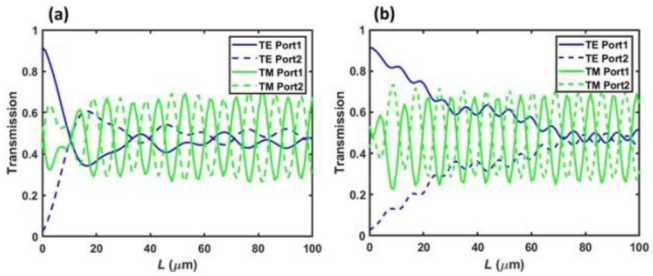

Fig. 3. Transmissions of port 1 and port 2 as a function of Region III length L for TE and TM modes. (a) MPAE-optimized 3-dB coupler. (b) Conventional adiabatic 3-dB coupler.

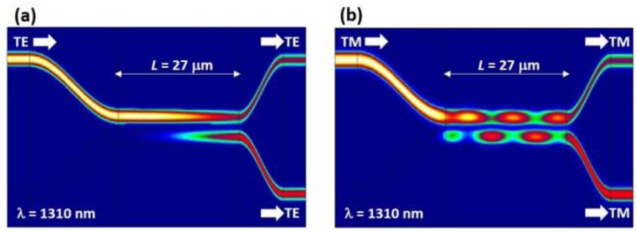

Fig. 4. Simulated light propagation in the MPAE-optimized 3-dB coupler with an $L = 27$ μm for the (a) TE mode and the (b) TM mode.

In the 10 μm long region IV, two S-bend waveguides of the same widths W_3 is used to separate the two waveguides from g_2 to g_1 to avoid additional optical mutual coupling. Finally, in the 5 μm long region V, two linear taper waveguides with widths varying from W_3 to W_0 are used. The physical parameters of the MPAE-optimized polarization-independent 3-dB coupler are summarized as follows: $W_0 = 0.38$ μm, $W_1 = 0.4$ μm, $W_2 = 0.3$ μm, $W_3 = 0.35$ μm, $g_1 = 3$ μm and $g_2 = 0.15$ μm.

We optimize and simulate the MPAE-optimized polarization-independent 3-dB coupler using a full-vectorial finite-difference mode solver and the eigenmode expansion method (EME) [24]. The MPAE process outlined in the previous section is used to obtain the optimized taper function $W(z)$ shown in Fig. 1(f). To determine the length L of the taper function, the device is simulated at 1310 nm of wavelength for both TE and TM polarizations. We simulate the light transmission for TE and TM polarizations at two output ports as a function of L, as shown in Fig. 3(a). The transmission curves for TE port 1, 2 (blue solid curve and dashed curve) and TM port 1, 2 (green solid curve and dashed curve) are nearly crossover at the length $L = 27$ μm. This means that the device can function as a polarization-independent 3-dB coupler at the length of $L = 27$ μm. Fig. 3(b) shows the TE and TM outputs of the conventional adiabatic polarization-independent 3-dB coupler with a linearly varying region III as a function of L. The transmission curves for TE port 1, 2 (blue solid curve and dashed curve) and TM port 1, 2 (green solid curve and dashed curve) are nearly crossover at the length of $L = 63$ μm, which is more than twice the length of the MPAE-optimized coupler. Therefore, MPAE can indeed shorten the length of mode evolution region and achieve polarization independence. We show the simulated light propagation in the device for TE and TM modes in Fig. 4, and the input light is equally split into port 1, 2 for both TE and TM modes. It is evident that the MPAE-optimized coupler achieves polarization-independent 3-dB coupling. We note that in Figs. 3 and 4, the TM results show strong oscillation. Even for the conventional adiabatic design in Fig. 3(b), the oscillation is still present even at long device lengths. The oscillation is due to a small excitation of the unwanted eigenmode at the beginning of the mode evolution region as shown in Fig. 4(b). Although MPAE is used to minimize unwanted coupling between the eigenmodes during mode evolution, the interference between the eigenmodes result in the observed oscillations. Excitation of the unwanted eigenmode can be reduced by further optimization of W_1, W_2, and g_2 in the design.

IV. Fabrication and Experimental Results

The MPAE-optimized 3-dB couplers were manufactured using MPW foundry service on an 8-inch SOI wafer by a CMOS-compatible process with ArF 193-nm deep ultraviolet lithography. The devices have upper and lower cladding of silicon oxide. Using a custom-built interrogation system, we characterize the

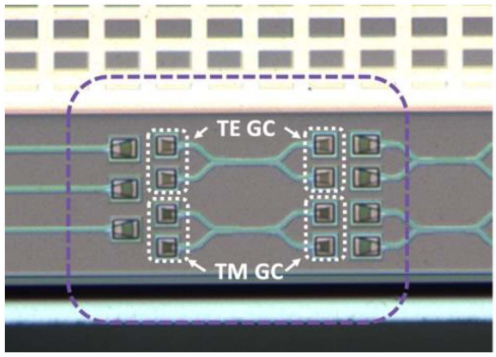

Fig. 5. Optical microscope image showing the fabricated MPAE-optimized 3-dB couplers with TE and TM grating couplers (GCs) attached for characterization.

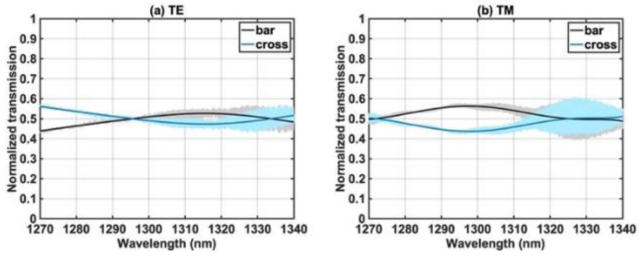

Fig. 6. Measured transmission spectra of the MPAE-optimized 3-dB coupler. (a) TE input. (b) TM input. The ripples in the responses are attributed to reflections from multiple interfaces in the characterization setup and the chip. To facilitate the estimation of the bandwidth, the spectral data are fitted with high-order polynomials, which are plotted in a bold black line and a bold blue line over the raw data.

spectral response of the fabricated couplers using a tunable laser with a tuning range of 1270 to 1340 nm and a step resolution of 1 pm [25]. Optical input/output between single-mode fiber and silicon chip is achieved using a pair of grating couplers having a coupler efficiency of −3.93/−4.14 dB for the TE and TM polarizations (Fig. 5). The output spectra at bar and cross ports of the MPAE-optimized 3-dB couplers for the TE [Fig. 6(a)] and the TM [Fig. 6(b)] polarizations are shown in Fig. 6. Measured optical spectra are normalized using the procedures outlined in [25] to remove the effect of coupling variation on the calculated power splitting ratio. For the TE mode, the maximum deviation from the designed 50/50 splitting ratio is 44/56 at 1270 nm. The maximum deviation is 56/44 at 1295 nm for the TM mode. The TM mode shows a larger variation in power splitting ratio across the wavelength range of interest as compared to the TE mode, which is consistent with the larger ripples in the TM mode transmission shown in Fig. 3(a). The polarization independent 3 ±0.5 dB bandwidth of the MPAE coupler is 70 nm (1270–1340 nm), limited by the bandwidth of the tunable laser and grating couplers.

V. Discussion and Conclusion

Recent advances in adiabatic guided wave optics have led to a more rigorous adiabatic criterion based on the local-mode theory [22]. In this work, we apply the MPAE process to engineer a heuristically defined adiabaticity parameter [23], which was successful in realizing compact and robust 3-dB couplers [14], [25]. The results presented in this work also demonstrate that polarization independent 3-dB couplers can be obtained using this metric. We note that the MPAE concept can also be applied to other measures of adiabaticity as long as their z dependence can be expanded by the chain rule similar to (1), with the possibility of considering more than one control parameters [22]. Comparing different adiabatic metrics will be a topic of future research and is beyond the scope of the current work.

In conclusion, we have proposed and demonstrated a compact and broadband polarization independent 3-dB coupler on SOI for the O-band. Short mode evolution length for dual polarization modes and multiple wavelengths is achieved by the newly introduced MPAE protocol. For both TE and TM polarizations, experimental results show that the MPAE-optimized coupler provides 3 ±0.5 dB splitting ratio for a wavelength range from 1270 nm to 1340 nm. The device is compatible with common silicon photonics foundry services.

Acknowledgment

The authors would like to acknowledge chip fabrication support provided by Taiwan Semiconductor Research Institute (TSRI).

References

[1] T. Tsuchizawa et al., "Microphotonics devices based on silicon microfabrication technology," *IEEE J. Sel. Topics Quantum Electron.*, vol. 11, no. 1, pp. 232–240, Jan./Feb. 2005.
[2] C. Sun et al., "Single-chip microprocessor that communicates directly using light," *Nature*, vol. 528, pp. 534–538, 2015.
[3] S. Chen, Y. Shi, S. He, and D. Dai, "Compact eight-channel thermally reconfigurable optical add/drop multiplexers on silicon," *IEEE Photon. Technol. Lett.*, vol. 28, no. 17, pp. 1874–1877, Sep. 2016.
[4] M. R. Watts, W. A. Zortman, D. C. Trotter, R. W. Young, and A. L. Lentine, "Low-voltage, compact, depletion-mode, silicon Mach–Zehnder modulator," *IEEE J. Sel. Topics Quantum Electron.*, vol. 16, no. 1, pp. 159–164, Jan./Feb. 2010.
[5] F. Horst, W. M. J. Green, S. Assefa, S. M. Shank, Y. A. Vlasov, and B. J. Offrein, "Cascaded Mach-Zehnder wavelength filters in silicon photonics for low loss and flat pass-band WDM (de-)multiplexing," *Opt. Exp.*, vol. 21, no. 10, pp. 11652–11658, 2013.
[6] H. Fukuda, K. Yamada, T. Tsuchizawa, T. Watanabe, H. Shinojima, and S. Itabashi, "Ultrasmall polarization splitter based on silicon wire waveguides," *Opt. Exp.*, vol. 14, no. 25, pp. 12401–12408, 2006.
[7] H. Xu and Y. Shi, "Ultra-compact polarization-independent directional couplers utilizing a subwavelength structure," *Opt. Lett.*, vol. 42, no. 24, pp. 5202–5205, 2017.
[8] L. Liu, Q. Deng, and Z. Zhou, "Subwavelength-grating-assisted broadband polarization-independent directional coupler," *Opt. Lett.*, vol. 41, no. 7, pp. 1648–1651, 2016.
[9] Y. Wang et al., "Polarization-independent mode-evolution-based coupler for the silicon-on-insulator platform," *IEEE Photon. J.*, vol. 10, no. 3, Jun. 2018, Art. no. 4900410.
[10] X. Chen, W. Liu, Y. Zhang, and Y. Shi, "Polarization-insensitive broadband 2×2 3 dB power splitter based on silicon-bent directional couplers," *Opt. Lett.*, vol. 42, no. 19, pp. 3738–3740, 2017.
[11] S. Longhi, "Quantum-optical analogies using photonic structures," *Laser Photon. Rev.*, vol. 3, no. 3, pp. 243–261, 2009.
[12] H.-C. Chung, S. Martínez-Garaot, X. Chen, J. G. Muga, and S.-Y. Tseng, "Shortcuts to adiabaticity in optical waveguides," *Europhysics Lett.*, vol. 127, no. 3, 2019, Art. no. 34001.

[13] V. Evangelakos, E. Paspalakis, and D. Stefanatos, "Efficient light transfer in coupled nonlinear triple waveguides using shortcuts to adiabaticity," *Sci. Rep.*, vol. 13, 2023, Art. no. 1368.
[14] Y.-J. Hung et al., "Mode evolution based silicon-on-insulator 3 dB coupler using the fast quasiadiabatic dynamics," *Opt. Lett.*, vol. 44, no. 4, pp. 815–818, 2019.
[15] H.-C. Chung and S.-Y. Tseng, "High fabrication tolerance and broadband silicon polarization beam splitter by point-symmetric cascaded fast quasiadiabatic couplers," *Opt. Continuum*, vol. 2, no. 10, pp. 2795–2808, 2019.
[16] H.-C. Chung, C.-H. Chen, Y.-J. Hung, and S.-Y. Tseng, "Compact polarization-independent quasi-adiabatic 2×2 3 dB coupler on silicon," *Opt. Exp.*, vol. 30, no. 2, pp. 995–1002, 2022.
[17] Y.-L. Wu, F.-C. Liang, H.-C. Chung, and S.-Y. Tseng, "Adiabaticity engineering in optical waveguides," *Opt. Exp.*, vol. 28, no. 20, pp. 30117–30129, 2019.
[18] H.-C. Chung, G.-X. Lu, and S.-Y. Tseng, "Shortcut to adiabaticity in silicon polarization splitter rotator using multi-wavelength adiabaticity engineering," *Opt. Exp.*, vol. 30, no. 5, pp. 8115–8125, 2022.
[19] H.-C. Chung and S.-Y. Tseng, "Ultra-broadband silicon polarization independent 3-dB coupler using multi-parameter adiabaticity engineering," in *Proc. IEEE Photon. Conf.*, 2022, pp. 1–2.
[20] J. D. Love, W. Henry, W. Stewart, R. Black, S. Lacroix, and F. Gonthier, "Tapered single-mode fibres and devices. Part 1: Adiabaticity criteria," *IEE Proc. J. (Optoelectron.)*, vol. 138, no. 5, pp. 343–354, 1991.
[21] S. G. Johnson, P. Bienstman, M. Skorobogatiy, M. Ibanescu, E. Lidorikis, and J. Joannopoulos, "Adiabatic theorem and continuous coupled-mode theory for efficient taper transitions in photonic crystals," *Phys. Rev. E*, vol. 66, no. 6, 2002, Art. no. 066608.
[22] D. F. Siriani and J.-L. Tambasco, "Adiabatic guided wave optics – a toolbox of generalized design and optimization methods," *Opt. Exp.*, vol. 29, no. 3, pp. 3243–3257, 2021.
[23] H.-C. Chung, K.-S. Lee, and S.-Y. Tseng, "Short and broadband silicon asymmetric Y-junction two-mode (de)multiplexer using fast quasiadiabatic dynamics," *Opt. Exp.*, vol. 25, no. 12, pp. 13626–13634, 2017.
[24] FIMMWAVE/FIMMPROP 7.2, Photon Design Ltd., 2022.
[25] Y.-J. Hung, C.-H. Chen, G.-X. Lu, F.-C. Liang, H.-C. Chung, and S.-Y. Tseng, "Compact and robust 2×2 fast quasi-adiabatic 3-dB couplers on SOI strip waveguides," *Opt. Laser Technol.*, vol. 145, 2022, Art. no. 107485.
[26] G. F. R. Chen, J. R. Ong, T. Y. L. Ang, S. T. Lim, C. E. Png, and D. T. H. Tan, "Broadband silicon-on-insulator directional couplers using a combination of straight and curved waveguide sections," *Sci. Rep.*, vol. 7, no. 1, 2017, Art. no. 7246.